Journal of Magnetism and Magnetic Materials 452 (2018) 415–426

Contents lists available at ScienceDirect

Journal of Magnetism and Magnetic Materials

journal homepage: www.elsevier.com/locate/jmmm

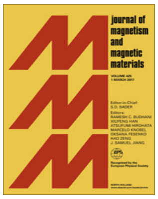

Research articles

Predictions of thermomagnetic properties of Laves phase compounds: $TbAl_2$, $GdAl_2$ and $SmAl_2$ performed with ATOMIC MATTERS MFA computation system

Rafał Michalski [a,*], Jakub Zygadło [b]

[a] Atomic Systems, M. Pszona 41/29, Cracow, Poland
[b] Faculty of Mathematics and Computer Science, Jagiellonian University, Cracow, Poland

ARTICLE INFO

Article history:
Received 19 May 2017
Received in revised form 16 November 2017
Accepted 18 December 2017
Available online 24 December 2017

Keywords:
$TbAl_2$
$GdAl_2$
$SmAl_2$
Crystal field
Atomic matters
CF
CEF
MFA

ABSTRACT

Recent calculations of properties of $TbAl_2$ $GdAl_2$ and $SmAl_2$ single crystals, performed with our new computation system called ATOMIC MATTERS MFA are presented. We applied localized electron approach to describe the thermal evolution of Fine Electronic Structure of Tb^{3+}, Gd^{3+} and Sm^{3+} ions over a wide temperature range and estimate Magnetocaloric Effect (MCE). Thermomagnetic properties of $TbAl_2$, $GdAl_2$ and $SmAl_2$ were calculated based on the fine electronic structure of the $4f^8$, $4f^7$ and $4f^5$ electronic configuration of the Tb^{3+} and Gd^{3+} and Sm^{3+} ions, respectively. Our calculations yielded: magnetic moment value and direction; single-crystalline magnetization curves in zero field and in external magnetic field applied in various directions $\mathbf{m}(T,\mathbf{B}_{ext})$; the 4*f*-electronic components of specific heat $c_{4f}(T,\mathbf{B}_{ext})$; and temperature dependence of the magnetic entropy and isothermal entropy change with external magnetic field – $\Delta S(T,\mathbf{B}_{ext})$. The cubic universal CEF parameters values used for all CEF calculations was taken from literature and recalculated for universal cubic parameters set for the RAl_2 series: $A_4 = +7.164\ Ka_0^4$ and $A_6 = -1.038\ Ka_0^6$. Magnetic properties were found to be anisotropic due to cubic Laves phase C15 crystal structure symmetry. These studies reveal the importance of multipolar charge interactions when describing thermomagnetic properties of real 4*f* electronic systems and the effectiveness of an applied self-consistent molecular field in calculations for magnetic phase transition simulation.

1. Introduction

One of the biggest challenges in materials science is understanding and controlling the microscopic quantum mechanisms responsible for controlling material entropy through external magnetic field change processes. Our calculation methodology makes it possible to describe the thermomagnetic properties of magnetic materials in large temperature scale such as: magnetic entropy, specific heat, single ionic magnetocrystalline anisotropy and magnetic moment direction and value of R ions (R = Rare Earth). Obtained thermomagnetic properties of materials are the consequence of thermal population of calculated Fine Electronic Structure of $4f^n$ electronic system of R^{3+} ions. We decided to test our approach for $TbAl_2$ $GdAl_2$ and $SmAl_2$ compounds. The material series RAl_2 compounds are intermetallic materials with interesting thermomagnetic properties [3]. In other words, the RAl_2 series of compounds are fascinating due to their large magnetocaloric entropy changes under external magnetic fields. This large change in MCE (Magnetocaloric Effect) is especially attractive in magnetic refrigeration due to its potential environmental friendliness compared to traditional gas refrigeration. We present results of simulations of thermomagnetic properties of some RAl_2 compounds performed with our new computation system called ATOMIC MATTERS MFA [1,2]. A few calculation results for $TbAl_2$ compound are compared with experimental data taken from the literature [3–6] and for $GdAl_2$ from papers [6,7]. All the lanthanides combine with aluminum to form RAl_2 compounds with the same crystalline structure [3]. All RAl_2 compounds are ferromagnetic at low temperatures [3]. RAl_2 crystals have the so-called cubic Laves phase C15 structure, while the point symmetry for rare earth ions is $43m$. The elementary cell of the crystal structure of Laves phase is presented in Fig. 1. The CEF (Crystal Electric Field) parameters describing the multipolar charge interaction of R ions in the crystal surrounding in this structure was agreed for all compounds and established according to studys of the $DyAl_2$ compound [3] for: $A_4 = +7.164\ Ka_0^4$ and $A_6 = -1.038\ Ka_0^6$. We decided to predict the properties of $TbAl_2$ and $GdAl_2$ completely without free parameters;

---

[*] Corresponding author.
E-mail address: r.michalski@induforce.eu (R. Michalski).

https://doi.org/10.1016/j.jmmm.2017.12.069
0304-8853/

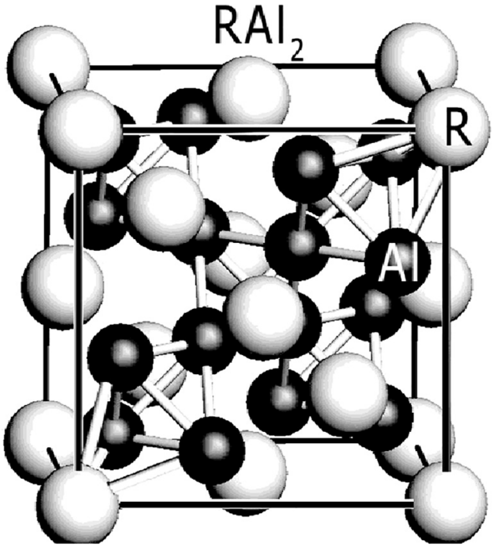

Fig. 1. Cubic elementary cell of RAl_2 Laves phase C15 crystals. Note: We present results of our calculations in atomic units ($a_o = 5.291772 \times 10^{-11}$ is Bohr radius). For convenient comparison of thermal properties of materials with electronic energy level structure of the R^{3+} ion, the energy unit is K (Kelvin); 1 K = 0.861733 meV = 1.38040×10^{-23} J.

therefore, we used the established cubic CEF and molecular field factor n_{mol} that were recalculated from $DyAl_2$.

2. Computation system

All calculations for $TbAl_2$ and $GdAl_2$ were performed with ATOMIC MATTERS MFA computation system. This extension of the ATOMIC MATTERS application [1] describes fine electronic structure and predicts basic magnetic and spectral properties of materials in a paramagnetic state. ATOMIC MATTERS MFA computation system [2] provides magnetic, calorimetric and spectroscopic properties of atomic-like localized electron systems under the influence of Crystal Electric Field (CEF), spin–orbit coupling and magnetic interactions, taken both as dynamic Mean Field Approximation (MFA) and the influence of established external magnetic field $\mathbf{B}_{ext}$ [2]. ATOMIC MATTERS MFA calculates macroscopic properties of materials in defined temperature regions, especially around the phase transition temperature: magnetic moment $\mathbf{m}(T,\mathbf{B}_{ext})$ (spin and orbital, directional components), localized electron specific heat $c_{4f}(T,\mathbf{B}_{ext})$, localized electron entropy with a useful tool set for MCE, isothermal entropy change $-\Delta S(T,\mathbf{B}_{ext})$ calculations, evolution of energy level positions, total free energy and more.

To enhance ease of use and efficiency, both calculation systems implement an advanced Graphic User Interface (GUI) with a system of hierarchical tabs for managing calculation results, 3D interactive visualizations of potentials and fields based on Open Graphics Library (OpenGL), intuitive tools and databases. More up-to-date information on features of Atomic Matters computation systems are available on our web page [8].

3. Theoretical background

ATOMIC MATTERS MFA computation system calculation methodology is deeply rooted in atomic physics. Taking into considerationindividual population of states of fine electronic structure of ions/atoms at different temperatures according to Boltzmann statistics makes it possible to define the temperature dependencies of single ionic properties. ATOMIC MATTERS MFA can simulate phase transitions of ionic/atomic systems according to dynamic calculations of the molecular field B_{mol}, simply defined as:

$$\mathbf{B}_{mol}(T) = n_{mol}\mathbf{m}(T) \tag{1}$$

which interacts with ions to induce their magnetic moments. Such self-consistent calculations can only be performed after establishing the molecular field factor n_{mol} that is closely related to the temperature of phase transitions, T_C.

For rapid calculations in a thermodynamically stable temperature region, ATOMIC MATTERS offers the following CEF + Spin-Orbit + Zeeman Hamiltonian according to the chosen calculation space of ground multiplet $|J,Jz>$ or ground atomic term $|LS,L_z,S_z>$, respectively [1]:

$$H_J = H_{CEF} + H_{Zeeman} = \sum_n\sum_m B_n^m \hat{\mathbf{O}}_n^m(J,J_z) + g_L\mu_B\mathbf{J}\cdot\mathbf{B}_{ext} \tag{2}$$

or

$$\begin{aligned} H_{LS} &= H_{CEF} + H_{S-O} + H_{Zeeman} \\ &= \sum_n\sum_m B_n^m \hat{\mathbf{O}}_n^m(L,L_z) + \lambda\mathbf{L}\cdot\mathbf{S} + \mu_B(\mathbf{L} + g_e\mathbf{S})\cdot\mathbf{B}_{ext} \end{aligned} \tag{3}$$

For all Hamiltonians B_n^m denote CEF parameters, $\mathbf{O}_n^m$ are Stevens operators, λ is the spin–orbit constant, and g_L and $g_e \approx 2.002319$ are the gyromagnetic factors of the whole ion or single electron, respectively, μ_B is the Bohr magneton and $\mathbf{B}_{ext}$ is the external magnetic field. In all cases, calculations in the $|LS,L_z,S_z>$ space are more physically appropriate due to their completeness, but traditional calculations in $|J,J_z>$ space can also be performed by our computation systems for comparisons and rapid estimations [2]. For calculating properties in temperatures around the magnetic phase transition point, a self-consistent methodology for molecular field calculation called Mean Field Approximations (MFA) is applied. The idea behind this method is to estimate the direction and value of the magnetic field (molecular field) generated by ions at a defined temperature, and to calculate the influence of this magnetic field for electronic state structures of ions. In a selected calculation space, according to Eq. (1) we define a molecular field as an expected value of the total moment of the 4*f* electronic subshell multiplied by the molecular field, inter ionic exchange factor n_{mol}:

$$\mathbf{B}_{mol} = -n_{mol}g_L\mu_B\langle\mathbf{J}\rangle \tag{4}$$

or

$$\mathbf{B}_{mol} = -n_{mol}\mu_B\langle\mathbf{L} + g_e\mathbf{S}\rangle \tag{5}$$

where the gyromagnetic factors are g_L and $g_e \approx 2.002319$. On the basis of the calculated electronic level structure $E_i(T)$, the directional components of magnetic moments are established for all described ions. This means that Hamiltonian matrix diagonalization is performed for all defined temperature steps recurrently. This is in contrast to simple ATOMIC MATTERS calculations [1], which diagonalize one matrix in a single run and deduce all thermodynamic properties from the stable discrete energy level structure obtained. This self-consistent procedure provides temperature-dependent energy level structure and has only one free parameter, n_{mol}, called the molecular field parameter. The value of n_{mol} is closely related to the phase transition temperature T_C of the macroscopic structure of ions. The formal expression of the full Hamiltonian used by ATOMIC MATTERS MFA computation system, according to the chosen calculation space: $|J,J_z>$ or $|LS,L_z,S_z>$, respectively, has the form:

$$\begin{aligned} H_{J\,mol} &= H_J + H_{mol} \\ &= +\sum_n\sum_m B_n^m \hat{\mathbf{O}}_n^m(J,J_z) + n_{mol}g_L^2\mu_B^2\left(-\mathbf{J}\langle\mathbf{J}\rangle + \frac{1}{2}\langle\mathbf{J}\rangle^2\right) + g_L\mu_B\mathbf{J}\cdot\mathbf{B}_{ext} \end{aligned} \tag{6}$$

or

$$\mathrm{H}_{\mathrm{LS\ mol}} = \sum_n \sum_m \mathrm{B}_n^m \hat{\mathbf{O}}_n^m(\mathrm{L},\mathrm{L}_z) + \lambda \mathbf{L}\cdot\mathbf{S} + n_{\mathrm{mol}}\mu_B^2\left(-(\mathbf{L}+\mathrm{g_e}\mathbf{S})\langle \mathbf{L}+\mathrm{g_e}\mathbf{S}\rangle + \frac{1}{2}\langle \mathbf{L}+\mathrm{g_e}\mathbf{S}\rangle^2\right) + \mu_B(\mathbf{L}+\mathrm{g_e}\mathbf{S})\cdot\mathbf{B} \tag{7}$$

The eigenvectors of the Hamiltonian are described, according to the selected calculation base, by the total momentum quantum numbers $|\mathrm{J},\mathrm{J}_z>$ or spin and orbit quantum numbers $|\mathrm{LS},\mathrm{L}_z,\mathrm{S}_z>$. Using the commutation relations of the angular momentum operators, we obtain information about expected values of the projections of magnetic momentum of all electronic states at a chosen temperature [2]:

$$\mathrm{m}_{\mathrm{J}}^{\alpha}(\mathrm{T}) = \frac{\mathrm{g_L}\mu_B}{\mathrm{Z(T)}}\sum_i \langle \mathrm{J}_{\alpha}^i\rangle \exp\left(-\frac{\mathrm{E}_i(\mathrm{T})}{\mathrm{k_B T}}\right) \tag{8}$$

$$\mathrm{m}_{\mathrm{LS}}^{\alpha}(\mathrm{T}) = \frac{\mu_B}{\mathrm{Z(T)}}\sum_i \langle \mathrm{L}_{\alpha}^i + \mathrm{g_e}\mathrm{S}_{\alpha}^i\rangle \exp\left(-\frac{\mathrm{E}_i(\mathrm{T})}{\mathrm{k_B T}}\right) \tag{9}$$

where α indexes directional components, *i* numbers the Hamiltonian eigenstates, while Γ_i represents the expected value of the total angular momentum along the α-axis in the *i*-th state:

$$\langle \mathrm{J}_{\alpha}^i\rangle = \langle \Gamma_i(T)|\mathrm{J}_{\alpha}|\Gamma_i(T)\rangle \tag{10}$$

$$\langle L_{\alpha}^i + g_e S_{\alpha}^i\rangle = \langle \Gamma_i(T)|L_{\alpha}^i + g_e S_{\alpha}^i|\Gamma_i(T)\rangle \tag{11}$$

All calculations of properties can be done in full 3D (x,y,z) real space using complex Hamiltonian matrix elements defined by full expressions of extended Stevens $\mathbf{O}_n^m$ operators [9]. Mostly for comparison with traditional calculation results, ATOMIC MATTERS also offers 2D (x,z) calculation methodology of a simplified model of CEF interactions defined by Stevens $\mathbf{O}_n^m$ operators with real number matrix elements only [10].

Taking into consideration the possibility of thermal population of states, we automatically obtain the thermal evolution of single ion properties of the whole compound [11,12].

Under the thermodynamic principle at the temperature of T = 0 K, only the ground state is occupied. In this situation, the magnetic moment of an ion is exactly equal to the momentum of the ground state. When the temperature rises, the probability of occupying higher states increases according to Boltzmann statistics. The number of ions with energy E_i within a system at temperature T is:

$$\mathrm{N}_i(\mathrm{T}) = \mathrm{N}_0\frac{\exp\left(-\frac{\mathrm{E}_i(\mathrm{T})}{\mathrm{k_B T}}\right)}{\mathrm{Z(T)}} \tag{12}$$

where $\mathrm{N}_0 \approx 6.022 \times 10^{-23}\ \mathrm{mol}^{-1}$ (Avogadro constant) and Z(T) is the statistical sum of states. Knowing the sum of states, we can determine the Helmholtz free energy F(T):

$$\mathrm{F(T)} = -\mathrm{k_B T}\ \ln \mathrm{Z(T)} \tag{13}$$

According to thermodynamic principles, the contribution of localized electrons to the total specific heat of materials can be calculated by taking second derivative of Helmholtz free energy:

$$\mathrm{c_{mol}(T)} = -\mathrm{T}\left(\frac{\partial^2 \mathrm{F(T)}}{\partial \mathrm{T}^2}\right) \tag{14}$$

This allows to calculate entropy according to the well-known definition:

$$\mathrm{S(T)} = \mathrm{S(0)} + \int_0^{\mathrm{T}} \frac{\mathrm{c(T)}}{\mathrm{T}}\mathrm{dT} \tag{15}$$

The value of electronic entropy for a defined temperature is difficult to compare, but the isothermal change of the entropy of the system at a given temperature is a very important material parameter that describes its thermomagnetic properties. Isothermal entropy change $-\Delta\mathrm{S}(\mathrm{T},\mathrm{B_{ext}})$, captured for different temperatures under the influence of different magnetic fields, is one the most important properties of a compound that describes its usefulness as a magnetocaloric material. The value $\Delta\mathrm{S}(\mathrm{T},\mathrm{B_{ext}})$, extracted from experimental specific heat measurements, is often presented as a basic description of the Magnetocaloric Effect (MCE) of a material [3–7]. In our approach, isothermal entropy change can be directly calculated from Eq. (15) according to the definition:

$$-\Delta\mathrm{S}(\mathrm{T},\mathrm{B_{ext}}) = \mathrm{S}(\mathrm{T},\mathrm{B_{ext}}=0) - \mathrm{S}(\mathrm{T},\mathrm{B_{ext}}) \tag{16}$$

ATOMIC MATTERS MFA also provides single-ionic magnetocrystalline anisotropy calculations that include full calculations (without Brillouin function approximation) of $\mathrm{K_i(T)}$ magnetocrystalline constants for defined temperature ranges according to the relations [15]:

$$\begin{aligned}
\mathrm{K_1(T)} &= \frac{3}{2}B_2^0(\langle\hat{\mathbf{O}}_2^0\rangle - \langle\hat{\mathbf{O}}_2^2\rangle) - 5B_4^0(\langle\hat{\mathbf{O}}_4^0\rangle - 3\langle\hat{\mathbf{O}}_4^2\rangle) - \frac{21}{2}B_6^0(\langle\hat{\mathbf{O}}_6^0\rangle - 5\langle\hat{\mathbf{O}}_6^2\rangle),\\
\mathrm{K_2(T)} &= \frac{35}{8}B_4^0(\langle\hat{\mathbf{O}}_4^0\rangle - 4\langle\hat{\mathbf{O}}_4^2\rangle + \langle\hat{\mathbf{O}}_4^4\rangle) + \frac{63}{8}B_6^0(\langle\hat{\mathbf{O}}_6^0\rangle - 20\langle\hat{\mathbf{O}}_6^2\rangle + 5\langle\hat{\mathbf{O}}_6^4\rangle),\\
\mathrm{K_2^*(T)} &= \frac{1}{8}(B_4^0\langle\hat{\mathbf{O}}_4^0\rangle + 5B_6^4\langle\hat{\mathbf{O}}_6^4\rangle)\\
\mathrm{K_3(T)} &= -\frac{231}{16}B_6^0\langle\hat{\mathbf{O}}_6^0\rangle, \mathrm{K_3^*(T)} = -\frac{11}{16}B_6^4\langle\hat{\mathbf{O}}_6^4\rangle.
\end{aligned} \tag{17}$$

where $\langle\hat{\mathbf{O}}_n^m\rangle$ denote thermal expected values of Stevens operators, defined according to C. Rudowicz [9]. The exchange interactions simulated with MFA methodology defined by Eq. (1) provide simulated properties strongly dependent on the only parameter nmol that is closely related to the temperature of phase transitions TC. It is easy to find the value of nmol for correct TC, but the value of this parameter can also be estimated according to De Gennes scaling [10]:

$$\mathrm{T_C} \sim \mathrm{G}(\mathrm{f^n}), \mathrm{G}(\mathrm{f^n}) = (\mathrm{g_L}-1)^2\mathrm{J}(\mathrm{J}+1) \tag{18}$$

De Gennes scaling is also a useful tool for $\mathrm{n_{mol}}$ estimation, as charge surroundings can be transferred between different ions in series. The CEF part of the Hamiltonian contains Stevens CEF parameters B_n^m and values of these parameters are only appropriate for the defined ion. The recalculation of B_n^m parameters defined for an ion A in the crystal lattice surrounding of ion B in the same crystalline position follows the simple scheme:

$$B_n^m(\mathrm{ion\ A}) \rightarrow A_n^m \rightarrow B_n^m(\mathrm{ion\ B}) \tag{19}$$

Stevens B_n^m parameters can be expressed by universal A_n^m parameters, according to the calculation space used, as follows:

$$\begin{aligned}
&|\mathrm{J},\mathrm{r}\rangle; B_n^m(\mathrm{J},\mathrm{J_z}) = \mathrm{q_n}(\mathrm{J})\langle r_{4f}^n\rangle A_n^m\\
&|\mathrm{LS},\mathrm{S_z},\mathrm{L_z}\rangle; B_n^m(\mathrm{L},\mathrm{L_z}) = \mathrm{q_n}(\mathrm{L})\langle r_{4f}^n\rangle A_n^m
\end{aligned} \tag{20}$$

Values$< \mathrm{r}_{4\mathrm{f}}^{\mathrm{n}}>$ of the 2nd, 4th and 6th power of average radius of the 4*f* shell have been calculated by many authors using Hartree-Fock-type methodology and the results can be easily found in the literature [13]. The θ_n parameters are the J- or L-dependent Clebsch-Gordan-type factors, sometimes called α,β,γ Stevens factors $\theta_2 = \alpha$, $\theta_4 = \alpha$, $\theta_6 = \gamma$, which can be expressed by finite equations available in [11–13]. The values of $<\mathrm{r}_{4\mathrm{f}}^{n}>$ are collected in the Atomic Matters system as an open database, together with a reference. In all presented calculations for R ions, we used the $<\mathrm{r}_{4\mathrm{f}}^{n}>$ values tabulated in [13]. The ability to recalculate CEF parameters between ions and calculation spaces offers a unique chance to establish an acceptable simplification of methodology. The recalculation of CEF parameters in Atomic Matters systems is fully automated, but an explicit Stevens Factors Calculator is also available.

4. Calculation results

In this section, we present the results of an investigation of the magnetic and magnetocaloric properties of a $TbAl_2$ and $GdAl_2$ single crystals. The predictions of properties are achieved completely without free parameters. We use established cubic CEF parameters for $DyAl_2$ in Stevens notation [3]: $B_4 = -(5.5 \pm 1.2) \cdot 10^{-5}$ meV and $B_6 = -(5.6 \pm 0.8) \cdot 10^{-7}$ meV. We recalculated these values of Stevens parameters to universal, ion-independent CEF notation A_n^m according to Eqs. (19) and (20). Therefore, we can assume that the parameters $A_4 = +7.164\ \mathrm{Ka}_0^6$ and $A_6 = -1.038\ \mathrm{Ka}_0^4$ obtained in this way define the charge surroundings of an R ion in a crystal lattice of RAl_2. The visualization of such defined potential is shown in Fig. 2. The triangular shapes, related with the location of the coordinating Al ions, are located symmetrically in cubic surroundings and reflect the atom position visible in the elementary cell of Laves phase shown in Fig. 2.

We attributed the magnetism of $TbAl_2$ to Tb and the magnetism of $GdAl_2$ to the Gd ions and performed calculations of the fine electronic structure of the $4f^8$ and $4f^7$ electronic systems, respectively. All calculations were performed for cubic symmetry, taking into account the crystal field and inter-site, spin-dependent exchange interactions. The energy level scheme derived is associated with the reduction of the degeneracy of the lowest atomic term (^2F and ^8S for Tb and Gd ions, respectively) given by Hund's first two rules. The value of molecular field factor n_{mol} for $TbAl_2$ and $GdAl_2$ was established according to $n_{mol}^{Dy} = 3.6\ T/\mu_B$ for $DyAl_2$ and de Gennes scaling Eq. (18) [10]. The comparison between experimentally found Curie temperature T_C and de Gennes scaling is shown in Fig. 3.

Experimental values of T_C for RAl_2 compounds [3–7] and the theory are in good agreement for 'heavy Rare Earths' elements from Gd ($4f^7$) to Yb($4f^{13}$). De Gennes relations [10,14] make it possible to establish molecular field factor for $TbAl_2$ $n_{mol}^{Tb} = 7.0\ T/\mu_B$ and for $GdAl_2$ $n_{mol}^{Gd} = 17.0\ T/\mu_B$. In case of Sm^{3+} ions the corresponding value of De Gennes factor is about 2 times smaller than deduced from T_C measurements and simple calculations of molecular field factor for $SmAl_2$ cannot be done and need special treatment that we present in Section 5.

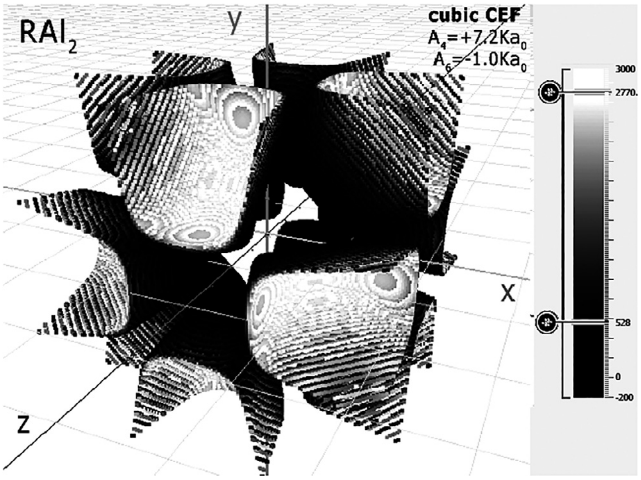

Fig. 2. Crystal Field potential visualization of cubic surrounding of R-ions in RAl_2, defined by CEF parameters: $A_4 = +7.164\ \mathrm{Ka}_0^4$ and $A_6 = -1.038\ \mathrm{Ka}_0^6$. The visualization of positive sign potential is externally cut off by the cube.

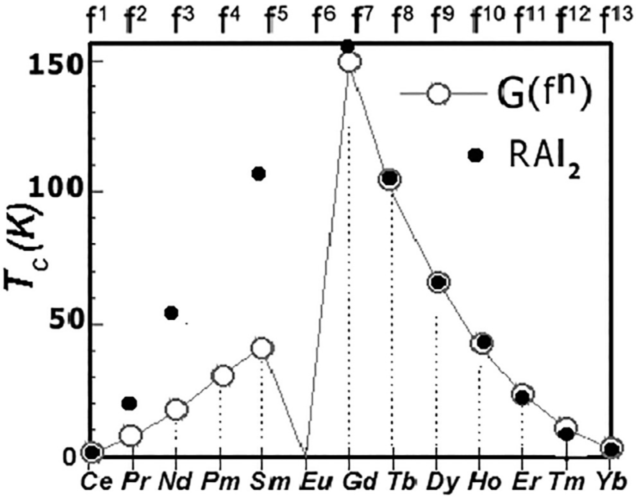

Fig. 3. De Gennes scaling of Curie temperature T_C for all rare-earth ions in series RAl_2 in comparison to experimental data from Ref. [3].

4.1. Calculated anisotropic properties of $TbAl_2$ single crystals

The $_{65}Tb$ atoms contain electronic structure that consists of a closed shell inactive atomic core [$_{54}Xe$], electronic system $4f^8$ and outer electrons $5d^1 6s^2$. We attributed the magnetic properties of $TbAl_2$ compound as an effect of properties of $4f^8$ electronic system under influence of electromagnetic interactions defined according to the description in the theory section. The starting point of our analysis is the ground atomic term ^2F with the quantum number of orbital angular momentum L = 3 and total spin S = 3.

The full calculated energy level structure in |LS,Lz,Sz> calculation space is shown in Fig. 4. The obtained overall splitting is strongly dependent on the strength of spin–orbit intra-atomic interactions. We used free-ion value of spin–orbit constant of Tb^{3+} ions $\lambda = -410$ K [13] and obtained overall splitting of ^2F atomic term at about 8620 K = 0.743 eV.

Details of a ground states structure are shown in Fig. 5. In the absence of an external magnetic field, the induced molecular field splits degenerated states. The value of the molecular field factor established for $TbAl_2$ which reproduces T_C well at about 105 K is $n_{mol} = 7.0\ T/\mu_B$.

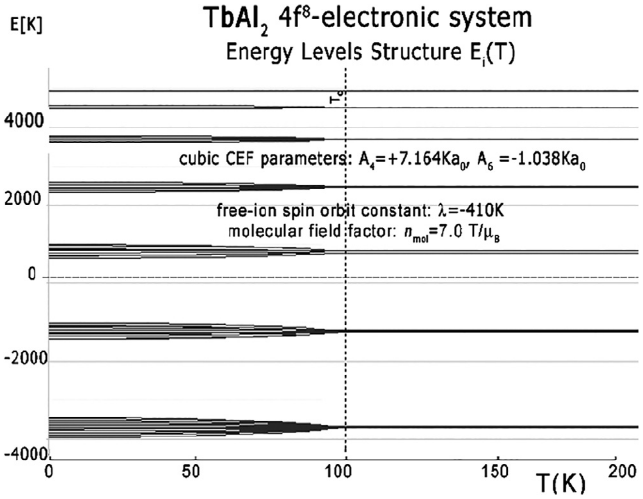

Fig. 4. The result of calculation of energy level positions vs. temperature of the fine electronic structure of $4f^8$ electronic configuration of Tb ions in $TbAl_2$ in |LS,Lz,Sz> space under the influence of intra-atomic spin–orbit coupling, inter-atomic self-consistent molecular magnetic field and Crystal Electric Field (CEF).

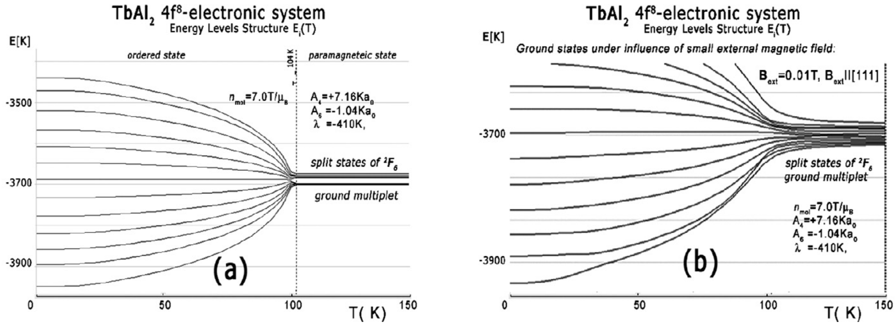

Fig. 5. The result of calculation of ground multiplet energy level structure vs. temperature. (a) Calculated states of the lowest multiplet of the fine electronic structure of $4f^8$ electronic configuration of Tb ions in $TbAl_2$ in |LS,Lz,Sz>. At Curie temperature T_C = 105 K the structure splits under the influence of molecular field. (b). Ground multiplet energy level structure vs. temperature under the influence of a small external magnetic field of 0.01 T applied along crystal direction [1 1 1].

Above T_C, in a paramagnetic state, the ground state is degenerated. The ground quartet consists of two quasi doublets. The wave functions of the ground state of Tb ($4f^8$ electronic system) ions in $TbAl_2$ in a paramagnetic state can be expressed in |Jz> notation as: $\Gamma_1 = +0.661|-4\rangle - 0.353|0\rangle + 0.6614|+4\rangle$ $\Gamma_2 = -0.151|-6\rangle - 0.691|-2\rangle + 0.691|+2\rangle + 0.151|+6\rangle$ $\Gamma_3 = -0.450|-3\rangle + 0.381|+1\rangle + 0.807|+5\rangle$ $\Gamma_4 = -0.450|+3\rangle + 0.381|-1\rangle + 0.808|-5\rangle$

A molecular field splits these states at $T < T_C$. The value of the molecular field changes, and at T = 0 (absolute zero) B_{mol} = 42 T and its direction is along the crystal [1 1 0] direction. In this condition, the wave function of a ground singlet gets the form: $\Gamma_0 = -0.358|-6\rangle + 0.567|-5\rangle - 0.553|-4\rangle + 0.407|-3\rangle - 0.247|-2\rangle + 0.122|-1\rangle - 0.04|0\rangle + 0.003|+1\rangle + 0.006|+2\rangle - 0.004|+3\rangle + 0.001|+4\rangle - 0.0002|+5\rangle + 0.0001|+6\rangle$

The electronic structure obtained in the absence of an external magnetic field is extremely fragile; even a small magnetic field applied along [1 0 0] or [1 1 1] direction forces the structure to change the order of states and creates an anomaly at low temperatures. The influence of a small external magnetic field applied along [1 1 1] direction for the structure of the lowest electronic states is shown in Fig. 5(b). The position of this anomaly corresponds with peaks on specific heat curves. The calculated specific heat for a $TbAl_2$ single crystal under the influence of an external magnetic field applied along various crystal directions is presented in Fig. 6.

The closer look at the unusual behavior of the 4*f*- electron component of specific heat simulated under the influence of an external magnetic field along 'diagonal' [1 1 1] direction is shown in Fig. 7 (a).

We have not found comparative experimental data for specific heat measurements, but F. W. Wang [5] provides data of measured specific heat change $\Delta c(T, B_{ext})$ defined as:

$$\Delta c(T, B_{ext}) = c(T, B_{ext}) - c(T, 0) \tag{21}$$

for measurements for ΔB_{ext} = 5T. Comparison between data from [5] and our simulations of $\Delta c(T, B_{ext})$ is shown in Fig. 7(b) The simulation for ΔB_{ext} = 5T in this figure is represented by a solid line.

Collected data of specific heat allows to calculate isothermal entropy change – $\Delta S(T, B_{ext})$ according to Eq. (16), the same methodology as used by experimentalists [3–7]. Isothermal entropy changes calculated with various external magnetic fields applied along all main directions of the cubic structure are presented in Fig. 8.

The anisotropic behavior of calculated thermomagnetic properties is reflected in magnetocrystalline anisotropy constant calculations. The results of $K_i(T)$ calculations according to Eq. (17) [16] in the absence of an external magnetic field are shown in Fig. 9.

For the sake of completeness, calculations of magnetic moment vs. temperature under various external magnetic field conditions were also performed. The graphs of $\mathbf{m}(T, \mathbf{B}_{ext})$ are presented in Fig. 10. The simulated thermal evolution of magnetic moment components under the influence of external magnetic field along [1 1 0] direction shown in Fig. 10(b) clearly confirms [1 1 0] direction as an easy magnetization axis of $TbAl_2$. The applied external magnetic field along this direction confirms perfect parallel directions of magnetic vector and external magnetic field (note: in cubic symmetry [1 1 0] = [0 1 1] = [1 0 1]).

Magnetic moment calculated in external magnetic field parallel to [1 1 1] and [1 0 0] direction reveals unusual behavior of the directional component of total moment. Similar behavior of magnetic moment directions was reported in [4], but most of the presented results of calculations of properties of $TbAl_2$ still await experimental verification. We found only a few reports about measurements of thermomagnetic properties of $TbAl_2$ single crystals. Some experimental comparative data of isothermal entropy change measured on $TbAl_2$ single crystals is provided by P.O. Ribeiro et al. [4,6], and interesting specific heat change measured on polycrystalline sample is provided by F.W. Wang at al. [5]. All experimental data from [3–6] confirms the correctness of our approach in predicting the thermomagnetic properties of $TbAl_2$.

4.2. Calculation of isotropic properties results for $GdAl_2$ crystals

The electronic configuration of Gd atoms consists of a closed shell inactive atomic core [$_{54}$Xe], a half filled 4*f* shell (e.g. electronic system $4f^7$), and outer electrons $5d^1 6s^2$. We attribute the magnetic properties of $GdAl_2$ compound to be an effect of properties of $4f^7$ electronic system under the influence of electromagnetic interactions defined according to the description in the theory section. The starting point of our analysis is the ground atomic term ^8S with the quantum number of orbital angular momentum L = 0 and total spin S = 7/2. This means Gd is a pure spin system. According to this, CEF does not interact with electronic states of the ground atomic term ^8S. In consequence, according to our approach, there is no source of single ionic anisotropy of Gd^{+3} ions with $4f^7$ electronic system. Inter-atomic magnetic interactions according to our MFA approach have pure isotropic nature Eqs. (4) and (5), therefore the obtained properties of $GdAl_2$ are absolutely identical despite the direction of the magnetic field applied. The value of molecular field factor n_{mol} for $GdAl_2$ was established according to de Gennes scaling [10] $n_{mol}^{Gd} = 17.0\ T/\mu_B$. The calculated energy level structure is shown in Fig. 11(a).

In the absence of an external magnetic field, the ground term of the $4f^7$ electronic system is fully degenerated. A self-consistent molecular field splits these states at $T < T_C$. The value of the

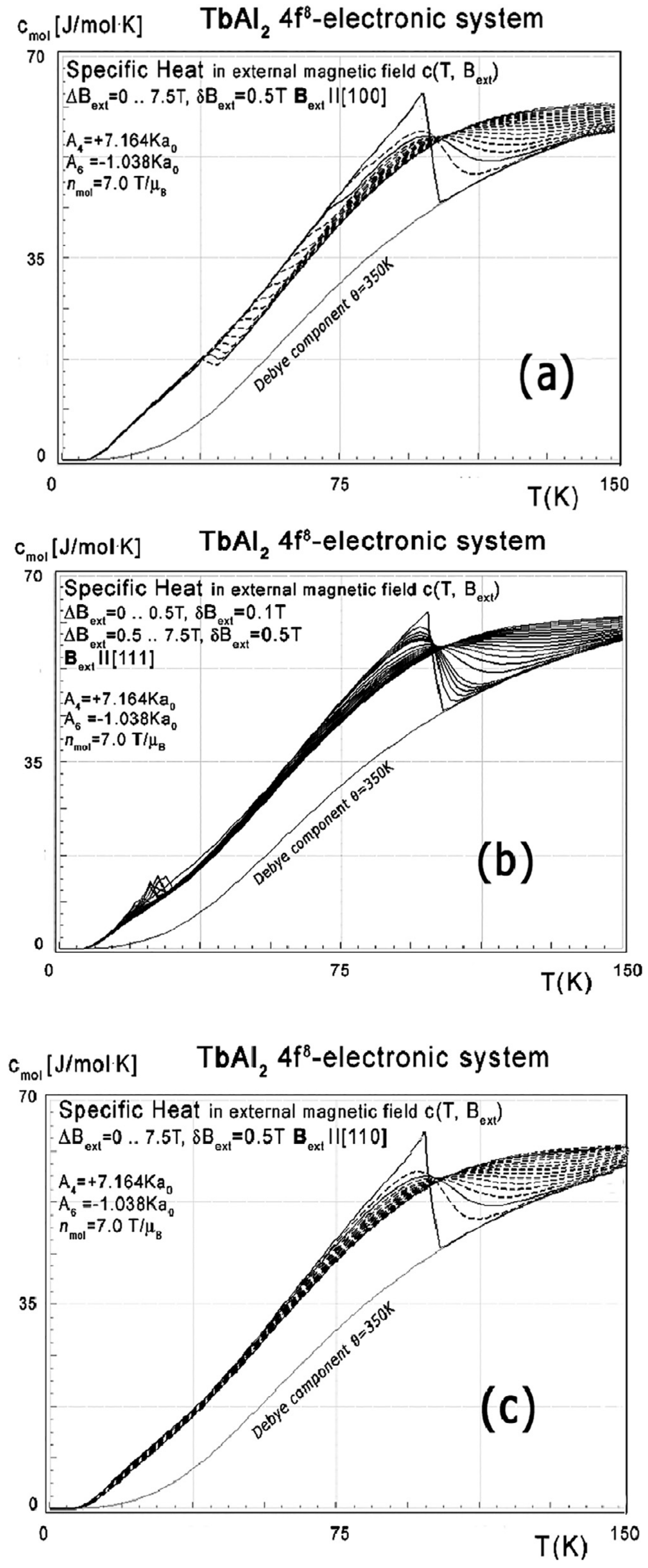

Fig. 6. Calculated 4*f*-electron component of molar specific heat (Eq. (14)) with Debye crystal lattice component (θ = 350 K) vs. temperature for Tb ions in TbAl$_2$, (a) under the influence of an external magnetic field applied along [1 0 0] direction. (b) under the influence of an external magnetic field applied along [1 1 1] direction. (c) under the influence of an external magnetic field applied along [1 0 0] direction.

molecular field changes, and at T = 0 (absolute zero) B_{mol} = 63 T. The influence of the external magnetic field B_{ext} = 6T on the structure of states is shown in Fig. 11(b).

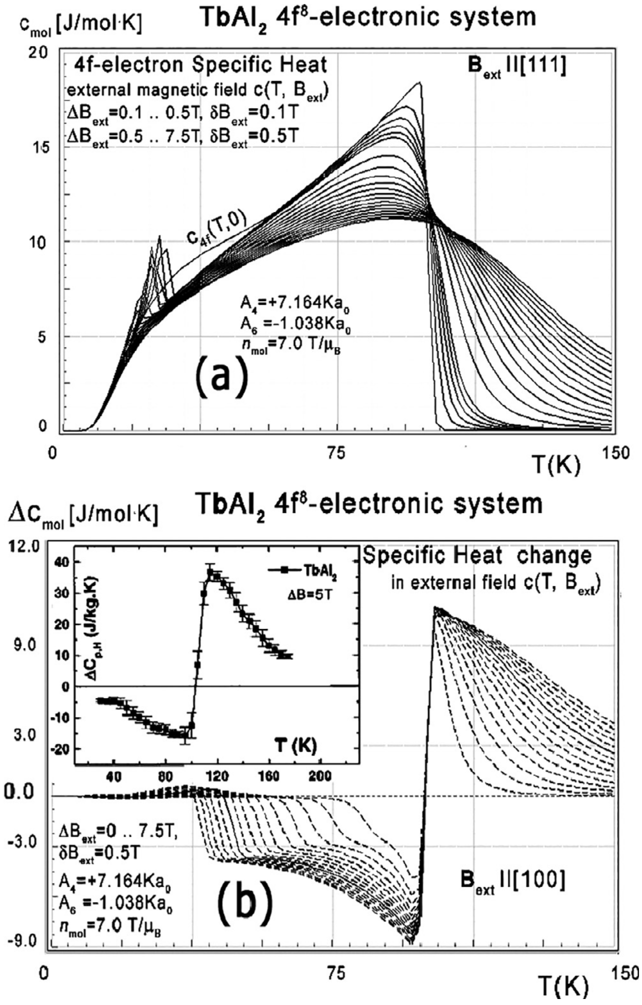

Fig. 7. (a). Calculated 4*f*-electron component of molar specific heat vs. temperature for Tb ions in TbAl$_2$, under the influence of an external magnetic field applied along [1 1 1] direction from 0 up to 7.5 T. (b). Calculated specific heat change vs. temperature for Tb ions in TbAl$_2$, under the influence of an external magnetic field applied along [1 0 0] direction from 0 to 7.5 T, with step 0.5 T in comparison with experimental data from [5]. Solid line represents simulation for ΔB_{ext} = 0.5 T.

The energy level structure makes it possible to calculate the 4*f*-electron component of specific heat. The result of calculation of specific heat under the influence of an external magnetic field compared to experimental data from Ref. [7] is shown in Fig. 12.

The calculations of electronic structure under the influence of an external magnetic field applied along [1 1 1] direction was also performed. The energy level structure calculated for the external magnetic field in this direction does not contain any anomaliels, as shown in Fig. 11(b). Specific heat calculated in this condition is shown in Fig. 12.

Collected specific heat data makes it possible to calculate isothermal entropy change – ΔS(T, B_{ext}) according to Eq. (16), the same methodology as used by experimentalists [3–7]. Isothermal isotropic entropy change calculated with various values of external magnetic field is presented in Fig. 13. The reference data taken from experimental measurement [3] is shown in the insets.

The isotropic behavior of calculated thermomagnetic properties agrees with experimental data [6,7]. For completeness, magnetic moment calculations vs. temperature under various external magnetic field conditions were performed – the results are presented in Fig. 14.

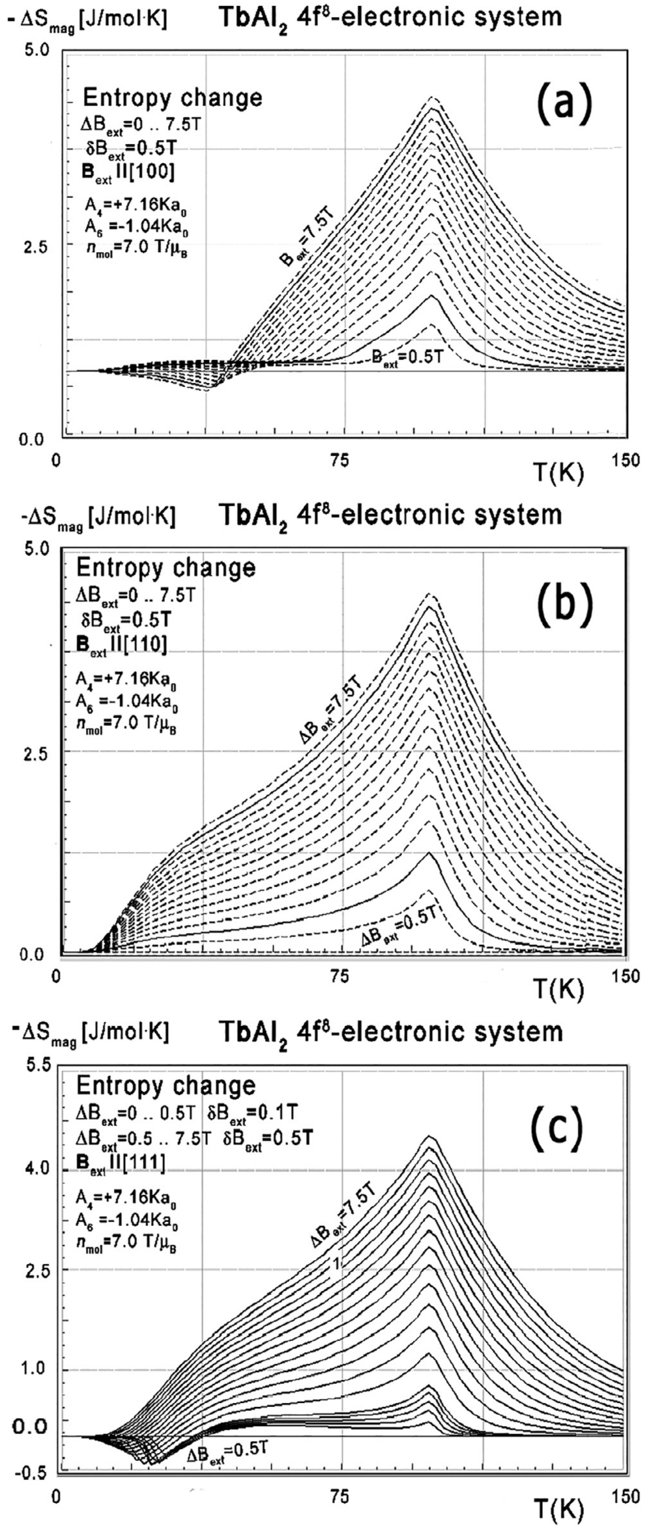

Fig. 8. Calculated isothermal entropy change of 4*f*-electronic system vs. temperature (Eq. (16)) of Tb ions in $TbAl_2$, under the influence of various external magnetic field values from 0 to 7.5 T, with step 0.5 T. (a). applied along [1 0 0] direction. (b). applied along [1 1 0] direction. (c). applied along [1 1 1] direction.

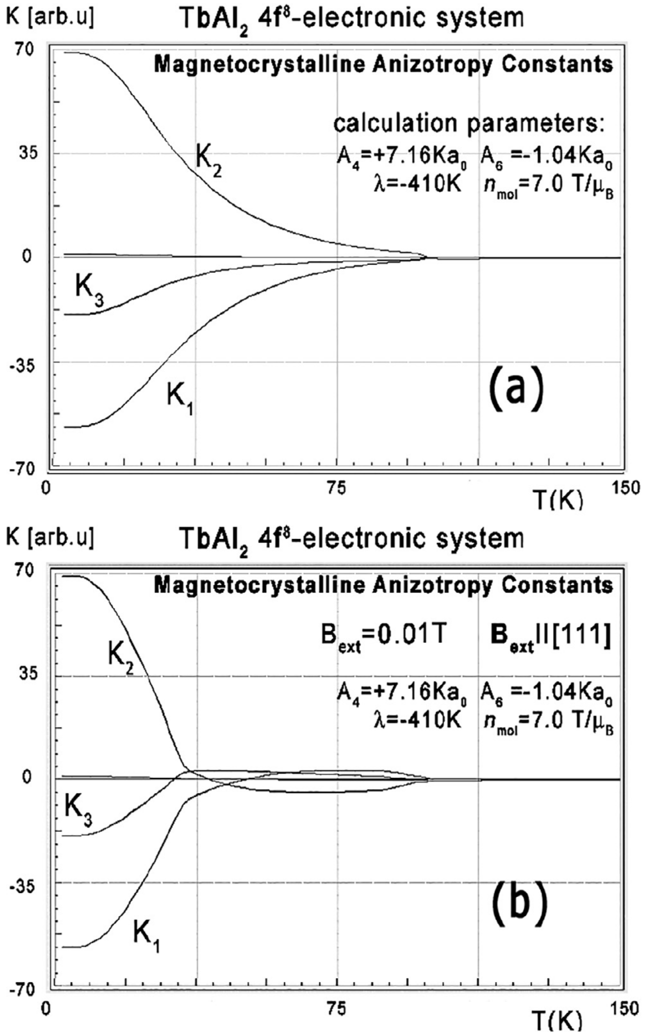

Fig. 9. Magnetocrystalline anisotropy constants K_1, K_2 and K_3 (calculated according to Eq. (17)) vs. temperature, for Tb ions in $TbAl_2$ in absence of an external magnetic field. (a). in absence external magnetic field, (b). Under the influence of small external magnetic field B_{ext} = 0.01 T, applied along [1 1 1] direction.

5. Calculation of properties of $SmAl_2$ single crystals

The local symmetry of coordinating charges of R^{3+} ions defines number of non-zero CEF parameters. In case of cubic crystal field, there are only two non-zero CEF parameters describing the coordinating potential. The relation between cubic CEF parameters B_4 and B_6 and generally defined CEF parameters used in Hamiltonians Eqs. (2), (3), (6) and (7) is simple:

$$B_4 = B_4^0 = 5B_4^0, B_6 = B_6^0 = -21B_6^4 \tag{22}$$

Universal A_n^m parameters, closely related to B_n^m was agreed for all compounds from the series [3]. CEF parameters with corresponding references, established for most RAl_2 compounds are collected in Table 1. We tested various combinations of values of A_n^m from the range covering whole span of values from Table 1: A_4: 5.0.0.23 Ka_0^{-4} and A_6: −0.3.−1.1 Ka_0^{-4} and we always obtained the same simulated magnetic characteristics of Sm ions in defined CEF. The value of CEF parameters for $SmAl_2$ was finally estimated according to RAl_2 lattice constants comparison: A_4 = +15 Ka_0^{-4} and A_6 = −1.0 Ka_0^{-6}.

The spin and orbital magnetic moments of the Sm ion under condition of defined CEF are found always antiparallel coupled and the magnitude of its orbital magnetic moment is always larger than that of the spin one. Calculations of electronic states in a paramagnetic state (ATOMIC MATTERS methodology) reveals this antiparallel coupling between spin and orbital momentum. The full structure of energy level in a paramagnetic state, calculated in

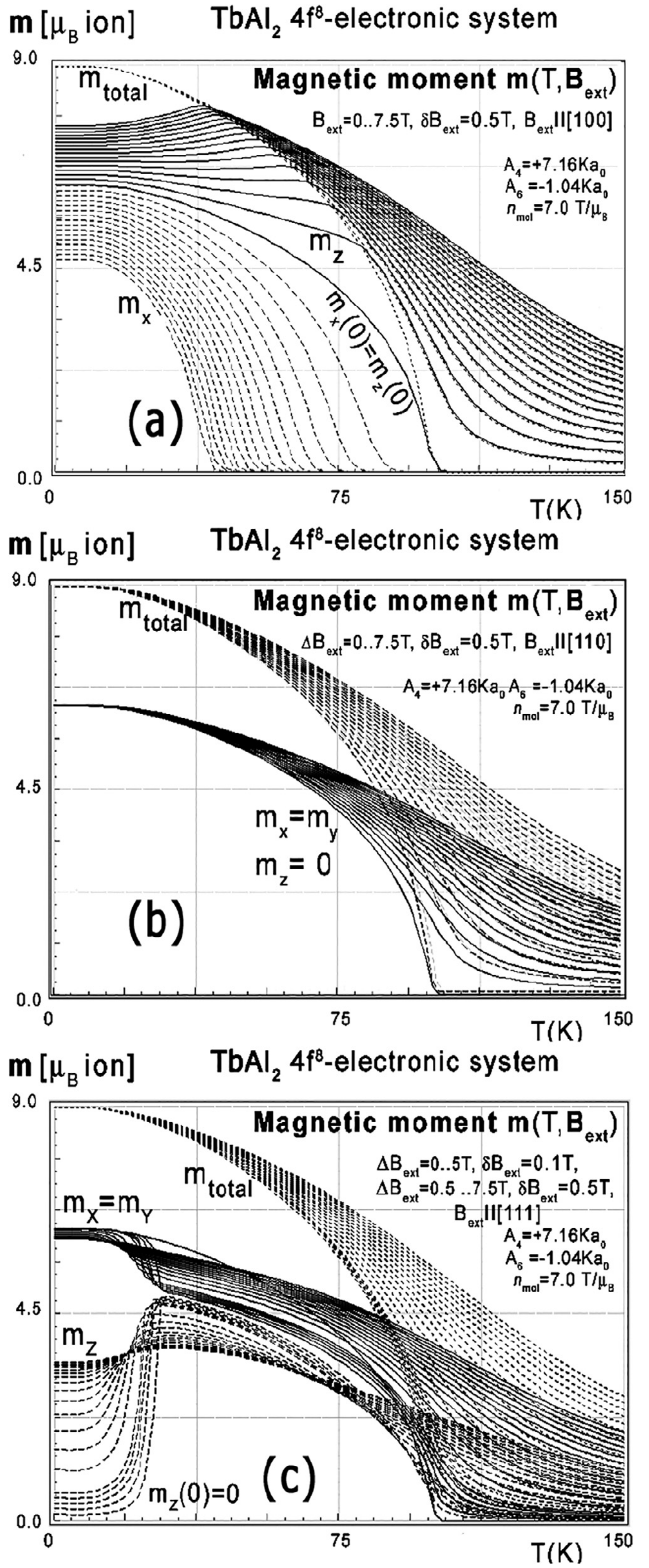

Fig. 10. Calculated x,y,z-directional components of total magnetic moment vs. temperature, calculated for Tb ions in TbAl$_2$ under the influence of CEF and molecular magnetic field and various values of external magnetic field from 0 to 7.5 T with step 0.5 T, (a) applied along [1 0 0] direction. (b) Applied along [1 1 0] direction. (c) applied along [1 1 1] direction.

|LS,L$_z$,S$_z$> space, together with expected values of angular momentum (spin and orbital) of particular states is shown in Fig. 15.

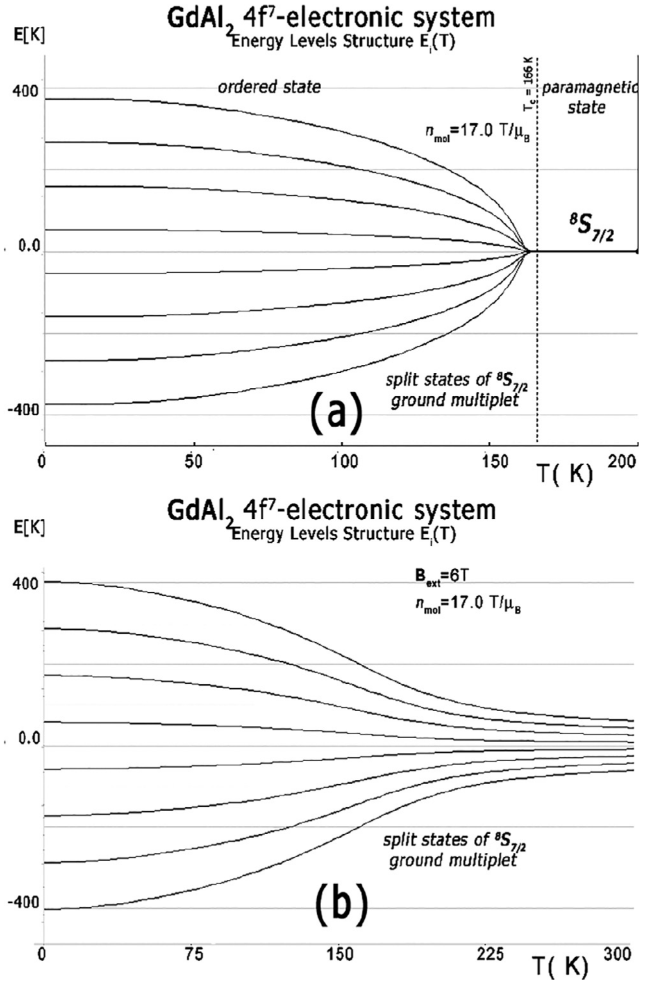

Fig. 11. (a). The result of calculation of energy level positions vs. temperature of the fine electronic structure of 4f^7 electronic configuration of Gd^{3+} ions in GdAl$_2$ under the influence of inter-atomic self-consistent molecular magnetic field and Crystal Electric Field (CEF). (b). Calculated energy level structure of 4f^7 electronic configuration of Gd^{3+} ions vs. temperature under the influence of external magnetic field 6 T.

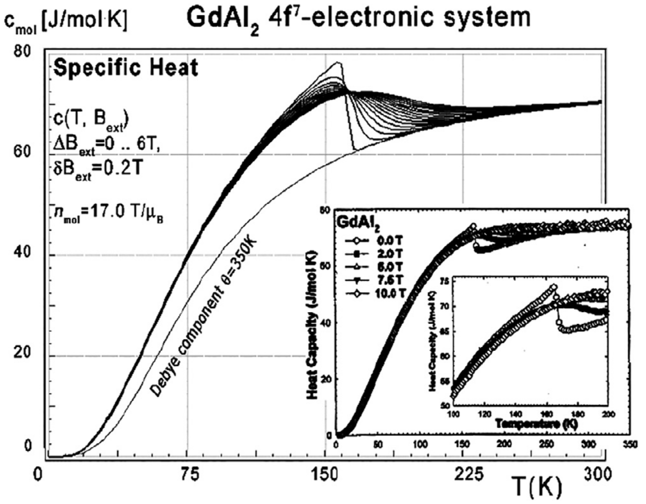

Fig. 12. Calculated 4f-electron component of molar specific heat (Eq.14) with Debye crystal lattice component (θ = 350 K) vs. temperature of Gd ions in GdAl$_2$, under the influence of external magnetic field from 0 to 6 T with step 0.2 T. Inset: experimental data from [7]

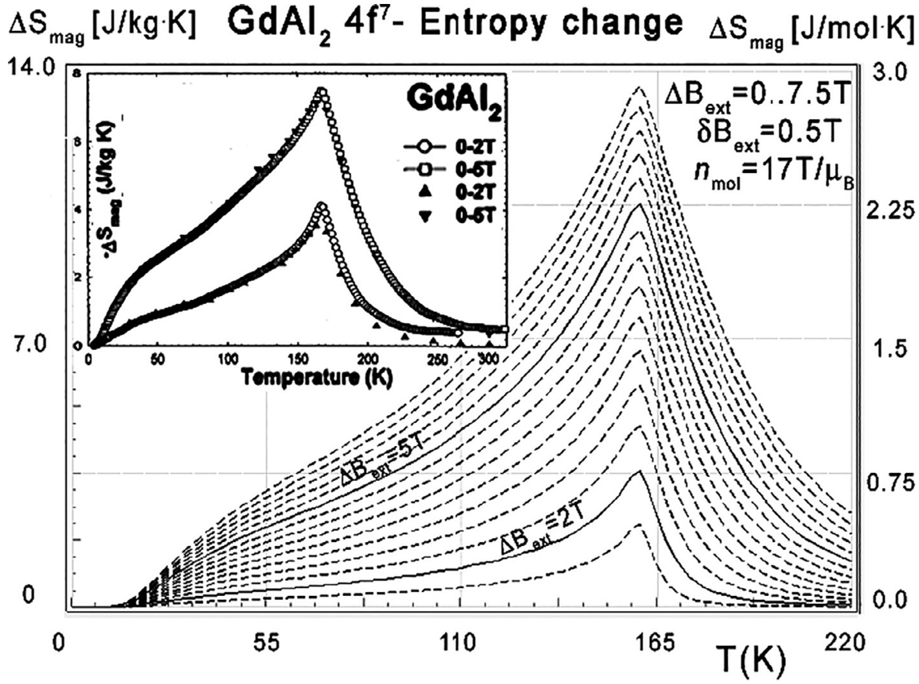

Fig. 13. Calculated isothermal entropy change of 4*f*-electronic system vs. temperature (Eq. (16)) of Gd ions in GdAl$_2$, under the influence of various values of external magnetic fields from 0 to 7.5 T, with step 0.5 T. Inset: isothermal entropy change obtained from experimental data, taken from [7]. Experimental data shown in inset corresponds with calculated solid curves for ΔB$_{ext}$ = 2 T and ΔB$_{ext}$ = 5 T.

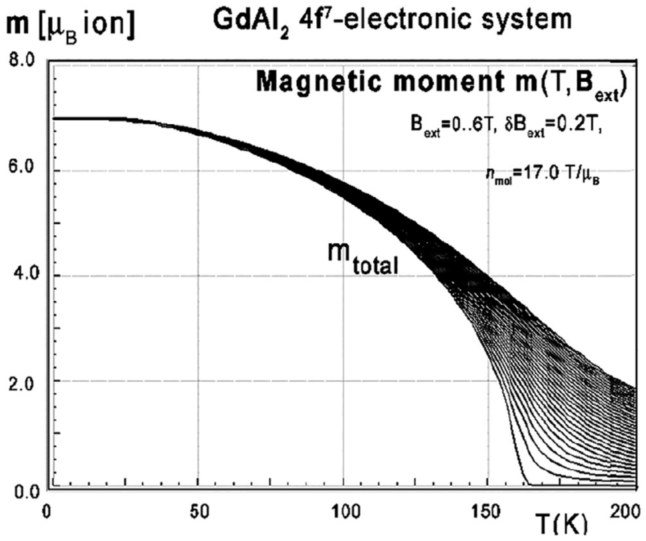

Fig. 14. Calculated uni-directional total magnetic moment vs. temperature, calculated for Gd ions in GdAl$_2$ under the influence of molecular magnetic field and various values of external magnetic field from 0 to 6.0 T with step 0.2 T.

The obtained electronic structure clearly demonstrates spin and orbital compensation of expected values of spin and orbital component of total angular momentum.

Calculations of energy level structure according to MFA methodology, in simplified |J,Jz> space, according to Eq. (6) (ground *J*-multiplet only) provide primitive energy level structure shown in Fig. 15(c). According to the described methodology we calculated the total moment **m**(T) under influence of molecular field (Fig. 16). To achieve Curie temperature T$_C$ of about 120 K, the value of the molecular field parameter was estimated at about n_{mol} = 950 T/μ$_B$. We do not have an explanation for such a large value of n_{mol}. The value of the ordered moment at T = 0 K achieved that way is approx. m(0) = 0.73 μ$_B$, about four times higher than the experimental value m$_{exp}$ = 0.2 μ$_B$ [17–22].

The energy level structure makes it possible to calculate localized electron specific heat under the influence of an external magnetic field, Fig. 17(a).

Collected data of specific heat makes it possible to calculate isothermal entropy change −ΔS(T, B$_{ext}$) according to Eq. (16). This is thesame methodology as used by experimentalist [4]. Isothermal entropy changes calculated with different values of external magnetic fields applied along the [0 0 1] direction of the cubic structure are presented in Fig. 17(b).

Table 1
The values of Cubic CEF parameters for RAl$_2$ series recalculated for |LS,L$_z$,S$_z$> and |J,J$_z$> space and related universal A_n^m parameters.

RAl$_2$	f^n	|JJz>		|LSLzSz>		universal		Ref.
R ion		B4 (meV)	B6 (meV)	B4 (K)	B6 (K)	A4 (Ka$_0^{-4}$)	A6 (Ka$_0^{-6}$)	
Pr	f^2	−4.40E−03	−8.80E−0.5	−5.10E−02	−1.02E−03	20.84	−0.912	[11]
Nd	f^3	−1.00E−03	4.00E−05	−1.6E−02	4.62E−04	13.69	−0.81	[11]
Sm	f^5	1.16E−04	2.24E−05	1.30E−02	2.60E−04	15	−1	(–)
Tb	f^8	3.00E−04	250E−07	3.48E−03	2.92E−06	17.2	−0.38	[11]
Dy	f^9	6.4E−05	−6.50E−07	6.50E−06	−6.38E−04	7.164	−1.038	[12]
Ho	f^{10}	−6.90E−05	6.40E−07	−7.99E−04	7.40E−06	17.4	−1.06	[11]
Er	f^{11}	1.10E−04	−1.30E−06	1.28E−03	−1.06E−05	22.63	−1.51	[11]

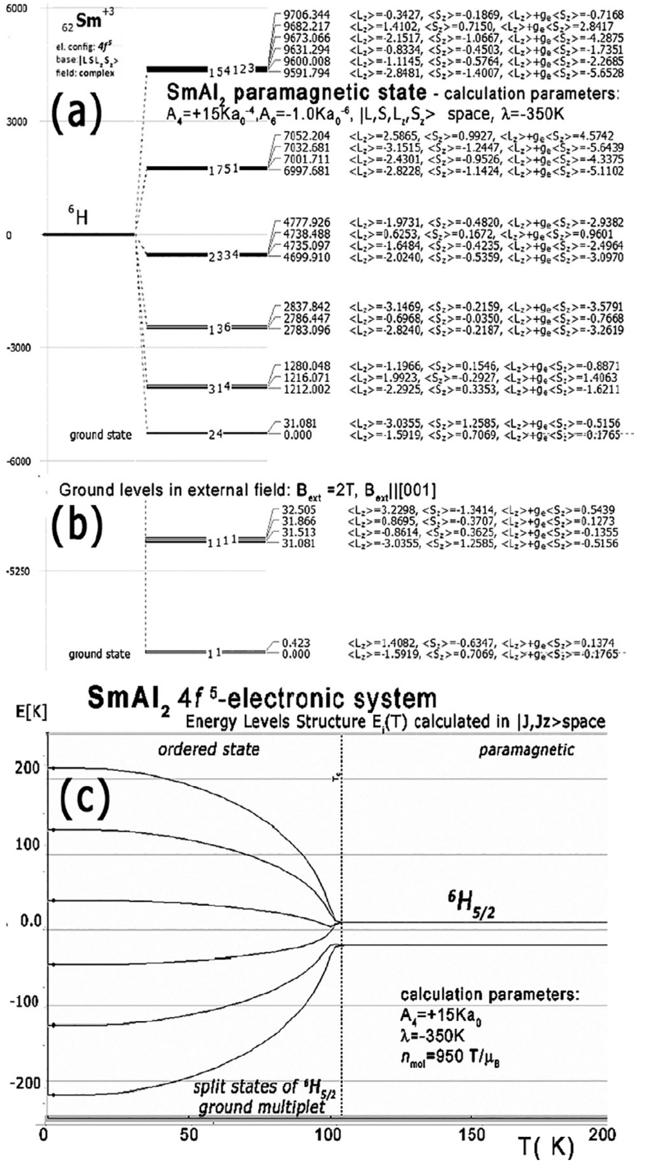

Fig. 15. (a) Energy level structure of Sm^{3+} ion $E_i(K)$ under the influence of defined CEF of $SmAl_2$ calculated in $|LS,L_z,S_z>$ space. (b) Lowest state of this structure, calculated under the influence of external magnetic field $B_{ext} = 2$ T applied along [0 0 1]. (c) Ground multiplet energy level structure vs. temperature calculated for $4f^5$ electronic system of Sm^{3+} in $SmAl_2$ calculated in |J,Jz> space.

Calculations of energy level structure according to MFA methodology in full $|LS,L_z,S_z>$ space does not provide expected effects. In every other case, calculations of magnetic properties of compounds from RAl_2 series collected in Tab.1 obtained in $|LS,L_z,S_z>$ space agreed better with experiment than simplified, but still conventional |J,Jz> space calculations. In the case of $SmAl_2$, calculation according to MFA methodology in $|LS,L_z,S_z>$ did not provide orderered state at all. Even using huge, unphysical values of $n_{mol} > 1000\ T/\mu_B$ cannot force the system to ordering. It is possible that other mechanism of magnetism coupling in $SmAl_2$ exists, which cannot be simulated by simple MFA methodology defined by Eq. (5). A possible mechanism of ordering involves spins or orbital moments separately. In such simulations the ordered moment of about ~0.2 μ_B is easy to obtain, but scientific correctness of such methodology needs more experimental evidences. The simulation of energy level structure of Sm^{3+} ions in $SmAl_2$ for orbital–only ordering mechanism is shown in Fig. 18.

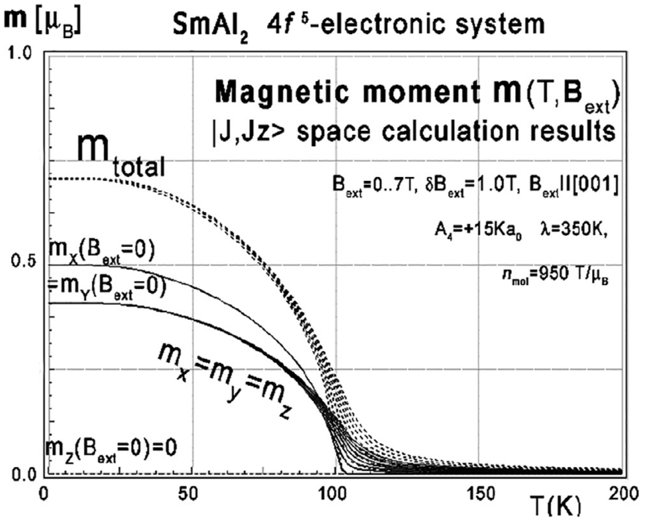

Fig. 16. Calculated x,y,z-directional components of total magnetic moment vs. temperature, calculated for $4f^5$ electronic system of Sm^{3+} in $SmAl_2$ calculated in |J,Jz> space.

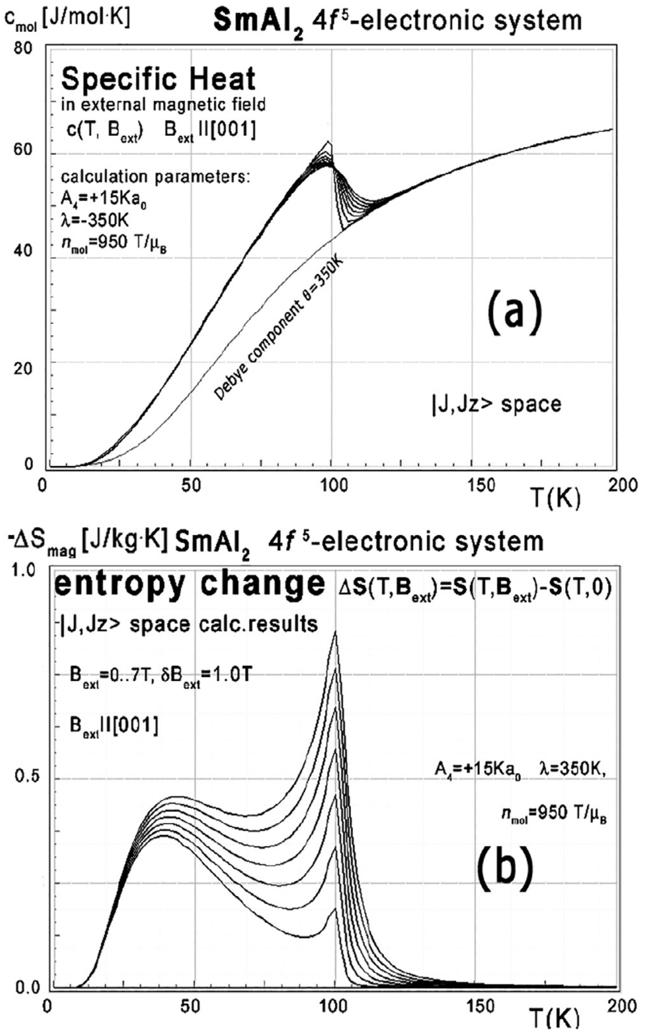

Fig. 17. (a) Calculated 4f-electron component of molar specific heat (Eq. (14)) with Debye crystal lattice component (θ = 350 K) vs. temperature for Sm^{3+} ions in $SmAl_2$, under the influence of an external magnetic field applied along [0 0 1] direction. (b) Calculated isothermal entropy change of 4f-electronic system vs. temperature (Eq. (16)) of Sm^{3+} ions in $SmAl_2$, under the influence of an external magnetic field from 0 to 7 T applied along [0 0 1] direction.

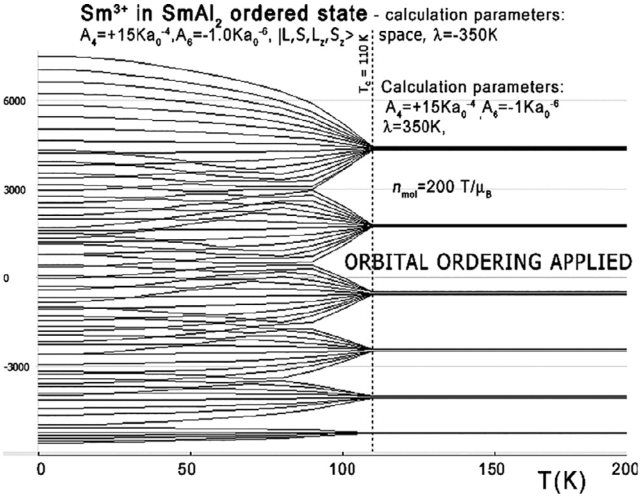

Fig. 18. The result of calculations of energy level structure vs. temperature for $4f^5$ electronic system of Sm^{3+} ions in $SmAl_2$ calculated according to orbital coupling in $|LS,L_z,S_z>$ space.

6. Conclusions

We performed calculations of electronic structure or localized 4*f* states of Tb^{3+}, Gd^{3+} and Sm^{3+} ions. Our calculations included influence of charge interactions of local surrounding of coordinating ions in $GdAl_2$, $TbAl_2$ and $SmAl_2$ compounds, respectively, and external magnetic field. In our approach we assume that the most fundamental magnetic properties of those compounds comes from R ions and single atomic properties of strongly correlated electronic system $4f^n$ plays predominantly role for magnetic behavior of the whole compound. We calculated the structure of eigenstates according to the methodology described in detail in Section 3. Populations of the excited states of the obtained structure of eigenstates e.g. Fine Electronic Structure, allows us to calculate thermomagnetic properties of considered materials such as: magnetic entropy, specific heat, single ionic magnetocrystalline anisotropy and magnetic moment direction and value. We have simulated entropy change with external magnetic field change applied along most important directions in crystals for all 3 compounds for wide range of temperatures from 0 K up to well above magnetic phase transition temperature.

All 3 compounds crystalize in the same crystal structure of Laves Phases C-15. We simulated the influence of the Crystal Field potential for the R^{3+} ions in this structure. The cubic local symmetry of R ions significantly simplifies the analyses, reducing the number of independent CEF parameters down to 2 (B_4 and B_6). We recalculated values of CEF parameters between isostructural RAl_2 compounds (according to Eqs. (19) and (20)), so all the calculations were performed without any free parameters. Some experimental data was compared with calculation results with very good agreement, but we do not find in literature the experimental data for most of our results, so it has to wait for experimental verification. Calculated magnetocrystalline anisotropy constants as well as specific heat of $TbAl_2$ reveal interesting, nonlinear behavior around 20–40 K (Figs. 6–8) in external magnetic field applied along [1 1 1] or [1 1 0] crystal direction. The reason of this behavior is the existence of two [1 1 0] and [1 1 1] directions of easy magnetization. The [1 1 0] direction is indeed an easy axis in lowest temperatures but small energetic difference between those magnetization directions is the reason of the reorientation of ordered moment between those directions under the influence of such weak magnetic field as $B_{ext} = 0.01$ T along [1 1 1] that is shown in the magnetocrystalline anisotropy plots for $TbAl_2$ in Fig. 9(a) and (b). This effect is the reason of creation of quasi-dublet on the bottom of the fine structure of electronic states under the influence of external magnetic field applied along [1 1 1], shown in Fig. 5(b). It makes the $TbAl_2$ material as a very interesting alternative for working material for magnetocaloric refrigerators and coolers working around temperature 100 K.

In case of Gd^{3+} in $GdAl_2$ all expectations of our calculations was confirmed. There is no single ionic magnetocrystalline anisotropy. The typical characteristics of magnetic entropy change behavior are in excellent agreement with experimental data shown in Fig. 13. $GdAl_2$ according to electronic configuration $4f^7$ of Gd^{3+} ions is a typical pure spin system which, according to Crystal Field theory, does not interact with crystal charge surrounding. This fact was fully confirmed by our results.

The $SmAl_2$ system reveals an interesting effect of spin moment and orbital moment compensation. Calculations of energy level structure according to MFA methodology in full $|LS,L_z,S_z>$ space do not provide expected results. In every other case, calculation of magnetic properties of compounds obtained in $|LS,L_z,S_z>$ space agreed better with experiment and were generally more valuable than performed in simplified, but still conventional $|J,Jz>$ space. In the case of $SmAl_2$, calculation according to MFA methodology in $|LS,L_z,S_z>$ did not provide orderered state at all. Even using huge, unphysical values of $n_{mol} > 1000\ T/\mu_B$ cannot force the system to ordering. It is possible that other mechanism of magnetism coupling in $SmAl_2$ exists, which cannot be simulated by simple MFA methodology defined by Eq. (5). A possible mechanism of ordering involves spins or orbital moments separately. In such simulations the ordered moment of about $\sim 0.2\ \mu_B$ is easy to obtain, but scientific correctness of such methodology needs more experimental evidence. We do not know the reason of this behavior and this effect needs further research.

Our results confirm the effectiveness of our theoretical approach. Working with ATOMIC MATTERS MFA revealed its high usefulness. The visual form of calculation results, full 3D interactive CEF potential visualization, intuitive tools for convention and unit recalculation, and the ability to compare all data results allow the user to utilize the power of the application very effectively. In conclusion, we confirm that ATOMIC MATTERS MFA is a unique application that combines a package of tools for correct description of the physical properties of atomic-like electron systems subjected to electromagnetic interactions in real materials. This is an accurate tool for calculating properties of ions under the influence of the electrostatic potential of ligands and both external (user defined) and internal inter-ionic magnetic fields..

References

[1] R. Michalski, J. Zygadło, Describing the Fine Electronic Structure and Predicting Properties of Materials with ATOMIC MATTERS Computation System, Proceedings: 18th Int. Conf. on Physics, Mathematics and Computer Science – Dubai, UAE, 2016, Available from: http://waset.org/publications/10004653/pdf.
[2] R. Michalski, J. Zygadło, Thermal dependences of single ionic, magnetic properties of materials in ordered state, calculated with ATOMIC MATTERS MFA computation system, in: Proceedings: 7th IIF-IIR International Conference on Magnetic Refrigeration at Room Temperature, Thermag VII – Torino, Italy, 2016.
[3] H.G. Purwins, A. Leson, Adv. Phys. 39 (1990) 309.
[4] P.O. Ribeiro, B.P. Alho, T.S.T. Alvarenga, E.P. Nóbrega, V.S.R. deSousa, A. Magnus, G. Carvalho, A. Caldas, N.A. de Oliveira, P.J. von Ranke, J. Magn. Magn. Mater. 379 (2015) 112–116.
[5] F.W. Wang, X.X. Zhang, F.X. Hu, Appl. Phys. Lett. 77 (9) (2000) 1360.
[6] P.O. Ribeiro, B.P. Alho, T.S.T. Alvarenga, E.P. Nóbrega, V.S.R. de Sousa, A. Magnus, G. Carvalho, A. Caldas, N.A. de Oliveira, P.J. von Ranke, J. Alloys Compd. 563 (2013) 242–248.
[7] S.Y. Dankov, V.V. Ivtchenko, A. Tishin, V.K. Pecharsky, Magnetocaloric effect in $GdAl_2$ and Nd_2Fe_{17}, conference paper, Adv. Cryogenic Eng. (Materials) 46 (2000), 397–404A.
[8] Software website: http://www.atomicmatters.eu.
[9] C. Rudowicz, C.Y. Chung, The generalization of the extended Stevens operators, J. Phys.: Condens. Matter 16 (2004) 5825–5847.

[10] P.G. de Gennes, J. Phys. Radiat. 23 (1962) 5010.
[11] M.T. Hutchings New York Solid State Phys. 16 (1964) 227.
[12] B.G. Wybourne, Symmetry Principles and Atomic Spectroscopy, J. Wiley and Sons, New York, 1970.
[13] A. Abragam, B. Bleaney, EPR of Transition Ions, Clarendon Press, Oxford, 1970.
[14] J.J.M. Franse, R.J. Radwanski, Magnetic properties of binary rare-earth, in: K.H.J. Bushow (ed.), Handbook of Magnetic Materials, Vol. 7, 1993, pp. 307–500.
[15] R.J. Radwański, R. Michalski, Z. Ropka, A. Blaut, Physica B 319 (2002) 78–89.
[16] B. Szpunart, P.A. Lindgard, J. Phys. F: Metal Phys. 9 (1979) 3.
[17] J.A. White, J.H. Van Vleck, Phys. Rev. Lett. 8 (1961) 412.
[18] M. Itou, A. Koizumi, Y. Sakurai, Appl. Phys. Lett. 102 (2013) 082403.
[19] S. Qiao, A. Kimura, H. Adachi, K. Iori, K. Miyamoto, T. Xie, H. Namatame, M. Taniguchi, A. Tanaka, T. Muro, S. Imada, S. Suga, Phys. Rev. B 70 (2004) 134418.
[20] H. Adachi et al., Phys. Rev. B 59 (1999) 11445.
[21] H. Adachi, H. Ino, Nature 401 (1999) 148–150.
[22] P.D. Kulkarni, S.K. Dhar, A. Provino, P. Manfrinetti, A.K. Grover, Phys. Rev. B 82 (2010) 144411. arXiv:1008.3779.